

新 制
理
448

京大附図

ポリパラキシリレンのエピタクシー合成

磯 田 正 二

Epitaxial Synthesis of  
Poly(p-xylylene)

Seiji Isoda

Institute for Chemical Research,  
Kyoto University, Uji, Kyoto 611, Japan

Key words Poly(p-xylylene);  
Epitaxy;  
Polymerization;  
Synthesis;  
Lattice Matching;  
Potential Calculation

## SYNOPSIS

When poly(p-xylylene) is synthesized from gaseous monomers, it grows epitaxially on substrates. The effects of the substrate and annealing on the epitaxy are examined by growing the polymer on cleavage (001) surfaces of four kinds of alkali halides (NaCl, KCl, KBr, KI). The polymer crystallizes with its chains oriented along the  $\langle 100 \rangle$  and  $\langle 010 \rangle$  directions of the substrates and the faster growth planes are parallel to the (001) plane of substrate, i.e., the (010) plane of the  $\alpha$ -form PPX and the (100) plane of the  $\beta$ -form. The degree of orientation is the highest on KBr and the lowest on NaCl. The lattice matching requirement is found to be important in the epitaxial synthesis. The observed orientation of polymer chain on each substrate is compared with the orientation expected from a minimum of interfacial potential energy calculated on the basis of dispersion-repulsive forces between atoms in the polymer and ions in the substrate. The orientational angle of polymer chain on the substrates and the degree of its orientation are qualitatively explained in terms of the processes of monomer deposition, polymerization and crystallization under the directive influence of substrate.

## 1. INTRODUCTION

Since Willems' and Fischer's works<sup>1,2</sup>, many studies have been reported on epitaxial crystallization of polymers. Most of them were concerned with the epitaxial growth of polymers on substrates from solutions by the isothermal immersion method<sup>3</sup>. Here a nucleated polymer crystal tends to arrange its chain axis parallel to the substrate surface so as to minimize the nucleation free energy, and a direction of faster crystal growth is normal to the substrate<sup>4</sup>. The relative geometry of polymer chains of several monomers with respect to the substrate was elucidated in particular in terms of interaction energy between a substrate and a single polymer chain<sup>5</sup>.

The long chain nature of polymers often prevents the sharp orientation of polymer crystals in epitaxial growth from solution. Contrary to this, the crystal orientation is expected to be well-defined in the case of epitaxial synthesis (or epitaxial polymerization) from gaseous monomers, i.e., polymerization of gaseous monomers and subsequent oriented crystallization on a substrate. The mechanism of epitaxy in polymerization from gaseous monomers should be simpler than from solution where the uncertain solvent effects<sup>3</sup> will complicate the situation.

of the epitaxy. Actually, the high degree of orientation was attained in the epitaxial polymerization of gaseous monomers, Nylon 6<sup>6</sup> and (SN)<sub>x</sub><sup>7</sup>. However, the details of the mechanism are not clear.

The present paper describes the epitaxial synthesis of poly(p-xylylene)  $(-\text{CH}_2-\text{C}_6\text{H}_4-\text{CH}_2-)_n$ , abbreviated to PPX) on alkali halides. PPX is most favourable for electron microscopic observation because of its excellent durability of crystallinity against electron bombardment<sup>8</sup> and it has been already known that the chains grow with their chain axes parallel to a surface of substrate when a glass is used as a substrate<sup>9</sup>. Here, the polymerization and subsequent crystallization of PPX took place on cleavage surfaces of single crystals of various alkali halides at room temperature. Through the electron microscopic observation of the polymer films thus obtained, the effects of the substrate and heat treatment on the crystal orientations on the substrate surfaces were examined and the mechanism of epitaxial polymerization is discussed.

## 2 EXPERIMENTAL

The synthesis of PPX was carried out according to Gorham's method<sup>10</sup>. Figure 1 shows the schematic drawing of the polymerization chamber. All reactions took place in a quartz tube in a vacuum of 0.1 Pa evacuated with a rotary pump. Dimer of p-xylylene in "Vaporizer" was evaporated at a temperature between 80°C and 100°C, and pyrolyzed at 650°C in "Pyrolysis". Gaseous monomers were polymerized and subsequently crystallized at 25°C on substrates in "Deposition". The thickness of PPX film on the substrate was controlled by changing the temperature and the evaporation time of dimer in "Vaporizer", and the films of 5-500 nm thickness were prepared. The thickness was directly measured by the electron microscopic observation of doubly folded PPX film which was previously covered with Pt-Pd.

It is well known that the temperature of substrates largely affects the epitaxy<sup>11</sup>. The temperature of the substrate was kept constant to 25°C for PPX, taking into account the extremely low rate of deposition at higher temperatures<sup>12</sup> and the metastable structure grown at lower temperatures<sup>13</sup>. The thermal effects on epitaxy were examined by successive annealing carried out without breaking the vacuum where the specimen in the quartz tube

directly transferred in the furnace of "Pyrolysis" kept at a temperature of annealing. The annealing time did not exceed 10 min in order to avoid the thermal degradation of PPX.

PPX was synthesized on the (001) plane of the freshly cloven surface of alkali halide single crystals; NaCl, KCl, KBr and KI. The PPX film was then floated off in distilled water and transferred to copper grids for electron microscopic observations. Electron diffraction patterns were taken with JEM-7A and JEM-200CS electron microscopes and the lattice images of PPX film were taken with a high resolution electron microscope JEM-500.

### 3. RESULTS

#### 3-1 As-polymerized PPX

The crystal structure of as-polymerized PPX is the  $\alpha$ -form<sup>14</sup>. Figure 2 shows the electron diffraction patterns obtained for as-polymerized PPX on four kinds of alkali halide. The thickness is approximately 40 nm for each specimen. Electron beams are perpendicular to the surface of PPX film. Two diffraction rings in each figure correspond to the 020- and 110-reflections of the  $\alpha$ -form PPX. Though the structure amplitude of 020 and 110 are the same order, the observed intensity of the 020-reflection is weaker than that of the 110-reflection. This shows that the b-axis is preferentially oriented normal to the surface of the PPX film. This b-axis orientation is consistent with the results obtained in the case on a glass substrate<sup>9</sup>. Moreover, the orientation of the 110-reflection suggests that the chain axis is oriented along the  $\langle 100 \rangle$  or  $\langle 010 \rangle$  direction of alkali halide, though the degree of orientation varies for each substrate. Thus, the molecular orientation of the polymer product is correlated with the direction of crystal axis of the substrate. Although the crystallinity of as-polymerized PPX is too low to estimate the orientation of the crystal with high



accuracy, the correlated orientation of the polymer is confirmed from the examination of annealed PPX, which is discussed in the next section.

When the thickness of PPX film exceeds 100 nm, the chain axis becomes less oriented along the  $\langle 100 \rangle$  or  $\langle 010 \rangle$  direction of the substrate. This deterioration of orientation will be due to the attenuation of the directive effect of the substrate on polymer chains far from it. As the thickness is reduced near to 5 nm, the decoration-like structures were frequently observed as shown in Figure 3. This suggests that the nucleation is initiated at steps on the substrate.

### 3-2 Annealed PPX

The epitaxial temperature (i.e., the substrate temperature) has a major effect on the orientation of deposits in epitaxy. The thermal effect on epitaxy was studied by annealing of PPX films on substrates in the present case. The  $\alpha$ -form transforms irreversibly to the  $\beta$ -form by annealing above ca.  $250^\circ\text{C}$ <sup>15</sup> where the chain direction is unchanged during the phase transition and the (010) plane of the  $\alpha$ -form coincides to the (100) plane of the  $\beta$ -form<sup>16</sup>

By annealing above  $300^\circ\text{C}$ , the crystallinity and

orientation of PPX were drastically changed. The electron diffraction patterns of PPX annealed at 380°C are shown in Figure 4 where the sample thickness is approximately 40 nm and the crystal structure changed to the  $\beta$ -form<sup>17</sup>. The main features of the orientation of crystals, i.e., the (100) plane of the  $\beta$ -form is parallel to the surface of substrates and the chain axis aligns along the  $\langle 100 \rangle$  or  $\langle 010 \rangle$  direction of substrates, are common for all cases and the highest degree of orientation is attained on KBr and the lowest on NaCl. In the images shown in Figure 4, the well-developed crosshatched structure is observed especially on KBr. The surface of the PPX film thicker than about 20 nm is originally smooth as observed at a low radiation dose of electrons, but a high dosage causes the crosshatched structure as shown in Figure 4 due to the deformation of an individual crystallite, which is considered to be a single crystal respectively. The lattice fringes due to the 001-reflection were observed sporadically in the PPX film annealed on KBr. These fringes align independently along either  $\langle 100 \rangle$  or  $\langle 010 \rangle$  direction of the substrate. Figure 5 shows an array of 0.655 nm lattice fringes observed in a crystallite.

Electron diffraction patterns (Figure 4) are indexed

by two patterns overlapped perpendicularly, one of which is shown in Figure 6-(b). The c-axis of the  $\beta$ -form aligns along the  $\langle 100 \rangle$  or  $\langle 010 \rangle$  direction of the substrate and the (100) plane of the  $\beta$ -form is parallel to the surface of the substrate (see Figure 6-(c)). This  $\beta$ -form orientation was proved experimentally, since the strong 040-reflection of the  $\beta$ -form was observed when the PPX film was tilted by  $30^\circ$  around the chain axis (i.e., the  $\langle 100 \rangle$  direction of substrate). The crystallographic relation between the  $\alpha$ - and  $\beta$ -forms confirms that the (010) plane of the  $\alpha$ -form in as-polymerized PPX should be parallel to the surface of substrate as shown in Figure 6-(a). The (010) plane of the  $\alpha$ -form and the (100) plane of the  $\beta$ -form are the faster growth planes, as seen in Figure 7.

By annealing at a higher temperature close to the melting point ( $T_m = 430^\circ\text{C}$ ), the thin smooth surface is changed into a rough block-like structure as revealed by Pt-Pd shadowing, and the orientation of crystals is extremely disturbed (see Figure 8). The moderate chain mobility is required to correlate the molecular orientation with the substrate, so that the annealing temperature will be restricted to a certain range. When the annealing temperature is lower than  $300^\circ\text{C}$ , the

molecular rearrangements will not take place to improve the crystallinity as well as the orientation of polymer chains with respect to the substrate. On the other hand, when annealed at a temperature higher than 400°C, the chain orientation is disturbed due to very high mobility of chains. At temperatures somewhat above 300°C the  $\beta_2$ -form of PPX appears<sup>18</sup>. Since the chains exercise thermal rotation freely in this temperature range, the  $\beta_2$ -form is considered as a pseudo-hexagonal structure similar to the rotator phase of paraffins. The excited thermal motions of molecular chains promote the molecular rearrangement and thus improve the crystallinity. However, as the temperature approaches to  $T_m$ , the higher chain mobility will eventually overcome the directive effect of the substrate on the molecular orientation.

In a few cases, the  $\underline{c}$ -axis of PPX happened to align also along the  $\langle 110 \rangle$  and  $\langle \bar{1}\bar{1}0 \rangle$  directions of KCl, KBr and KI.

## 4. DISCUSSION

### 4-1. Mechanism of epitaxy

The substrates define in some extent the morphology of polymer in the epitaxial synthesis of PPX and this extent depends on the nature of the substrates. The subsequent annealing improves the orientation of the crystal by increasing the chain mobility in the  $\beta_2$ -form. The origin of epitaxy will be discussed by considering four basic mechanisms of epitaxy<sup>11,19,20</sup> summarized below.

1) Some kind of long range force: The long range force mechanism has been proposed by Rybnikar et al.<sup>21</sup> in the case of polymers. They have emphasized the importance of this force from the observation that a deposit of poly- $\gamma$ -benzyle-L-gultamate maintains its morphological correlation with a substrate, even when the substrate is covered with thin carbon film in prior to crystallization. A similar experiment was carried out for PPX where PPX was synthesized and annealed on KBr covered with thin carbon or Al layer. Figure 9 shows that only the planar orientation of the c-axis takes place on the surface of substrate.

2). Nucleation control: As already shown in Figure 3, a number of crystallites are formed along curved steps

on the surface (i.e., decoration) and the nucleation is considered to be initiated at steps on the substrate.

3) Basal plane pseudomorphism in the initial layers of deposits: Pseudomorphic or intermediate phase in the initial layers of deposits was not observed in the present case in contrast to the cases of polyethylene, polyoxymethylene and polypropylene<sup>22</sup>

4) Geometrical fitting between the lattice of substrates and that of deposits: The lattice misfit was calculated as  $\text{misfit} = 100(c-a)/a$ , where  $c$  is the fiber period of PPX ( $c = 0.655 \text{ nm}$ ) and  $a$  the a-axis dimension of the alkali halides, considering the orientation of the c-axis along the  $\langle 100 \rangle$  direction of the substrate. The calculated misfit values are listed in Table 1 where the minimum value of misfit was obtained for KBr, the medium for KCl and KI, and the maximum for NaCl. These misfit values corresponds to the degrees of orientation as observed in Figures 2 and 4. The epitaxy in  $(\text{SN})_x$  is explained in terms of the multi lattice matching, i.e., the fit of  $m$  atom distances in a deposit with  $n$  atom distances in the parallel direction in a substrate<sup>23</sup> In  $(\text{SN})_x$  and PPX cases, the lattice matching is observed to be one-dimensional and the plane parallel to the surface of a deposit constitutes the faster growth plane. No

condition is fulfilled for the two-dimensional matching on the surface of the substrates<sup>24</sup>

As stated above, PPX nucleates at steps on the substrate and the orientation of chains is mainly determined by the lattice matching mechanism. Their orientation with respect to the substrate is enhanced by the increase of thermal motion of molecules as seen from the annealing effect. The plane of polymer crystal parallel to the surface of the substrate is considered to be that growing with the fastest rate. The growth planes are also the most densely packed planes of the  $\alpha$ - and  $\beta$ -form PPX.

#### 4-2. Potential calculation

The lattice control mechanism is dominant in the epitaxial growth of the present case, so that the dispersion-repulsive forces between atoms in the polymer and ions in the substrate define the orientation of polymer chain. That is, the polymers are oriented on the substrate so as to minimize the interfacial potential energy. The potential energy is to be calculated, assuming a Lennard-Jones type potential. Here the potential calculation is performed according to Mauritz et al.<sup>5</sup>, considering three types of deposits; (a) one

monomer, (b) one molecular chain composed of seven monomers, (c) three chains, each composed of seven monomers respectively. These deposits correspond to the monomer deposition, polymerization and crystallization processes, respectively. In all cases, the monomer or the chain aligns in the same positioning as in the (010) plane of the  $\alpha$ -form, which is parallel to the surface of the substrate. In this geometry the plane of benzene ring is perpendicular to the surface of the substrate. The geometrical relation between the polymer chain and the substrate is shown in Figure 10-(a). Here (u,v,h) denotes the coordinate of a center of a benzene ring in the polymer. The chain direction  $\phi$  is measured from the  $\langle 100 \rangle$  direction of the substrate. Parameters for calculation are u, v, h and  $\phi$ , since the b-axis orientation of the  $\alpha$ -form is assumed.

The energy contribution due to dispersion and repulsion can be described by a 6-12 potential,

$$U_{ij} = -\frac{A_{ij}}{r_{ij}^6} + \frac{B_{ij}}{r_{ij}^{12}}, \quad (1)$$

where  $r_{ij}$  is the distance between Atom i in the polymer chain and Ion j in the alkali halide.  $A_{jj}$  for like ion pair have been determined by Mayer<sup>25</sup> and  $A_{ij}$  is



calculated from the combination rule<sup>26</sup>,

$$A_{ij} \approx (A_{ii}A_{jj})^{\frac{1}{2}} \quad (2)$$

The corresponding values of  $B_{ij}$  can be calculated by imposing the condition that  $U_{ij}$  takes a minimum at the equilibrium distance, which is the sum of the van der Waals' <sup>27</sup> and ionic radii<sup>28</sup> for the atoms and ions, respectively. The 6-12 potential constants thus obtained for atom-ion pairs are listed in Table 2.

The summation can not be taken over all pairs of  $i$ -atoms and  $j$ -ions, and covers only a hemisphere region of radius  $R$ , as shown in Figure 10-(b). The remaining area is treated as a continuum<sup>5</sup>. The potential energy is given for the remaining area as

$$U_i = - \frac{\pi}{2R^3} \left( \frac{R-h}{R} + \frac{1}{3} \right) \int_s n(s)A(s) + \frac{\pi}{5R^9} \left( \frac{R-h}{R} + \frac{1}{9} \right) \int_s n(s)B(s), \quad (3)$$

where  $n(s)$  denotes the concentration of the  $s$ -kind (positive or negative) ion in substrates, and  $A(s)$  and  $B(s)$  are the attractive and repulsive force constants between  $i$ -atom and  $s$ -kind ion, respectively. When the

quantity  $R$  exceeds 1.0 nm, the potential energy is practically unchanged and thus 1.5 nm is allocated to  $R$  in the calculation.

The potential map is calculated with respect to  $(h,\phi)$  where the point  $(u,v)$  moves around in a shaded region shown in Figure 10-(c). For all substrates, the lowest value of the potential minima for all  $(u,v)$  is obtained at the contact point of positive and negative ions,  $P$  in Figure 10-(c). The maps thus obtained are shown in Figures 11, 12, 13 and 14 for each substrate. These maps explain qualitatively the correlated orientation between the molecules and the substrate as observed. The values of  $(h,\phi)$  which give the potential minima and the value of the potential minimum for each substrate are tabulated in Table 3.

Figures (a) in Figures 11-14 denote potential map when one monomer deposits on respective substrate, indicating that the chain direction makes an angle of about  $13^\circ$  with the  $\langle 100 \rangle$  direction of the substrate and then the plane of benzene ring should align exactly along the  $\langle 100 \rangle$  direction of the substrate. In the case of NaCl, the minimum is shallower than in any other case and this is the principal reason for the worst orientation observed on NaCl. For other substrates, the minima take

approximately the same values.

The potential map shown in (b) of each figure corresponds to the stage that the monomers are polymerized. A potential minimum is not well-defined in the case of NaCl, while the well-defined minimum exists at the orientation of  $\phi=0^\circ$  in other cases where the deepest minimum is observed in KBr. This minimum at the orientation of  $\phi=0^\circ$  shows that the chain axis tends to align along the  $\langle 100 \rangle$  direction of the substrates. The orientation of the PPX crystallite may be mainly determined in this stage. The minimum value of the potential well corresponds to the degree of orientation observed experimentally. In a few cases, the chain of PPX happened to orient also along the  $\langle 110 \rangle$  direction of the substrate. This corresponds to the shallow minimum at  $\phi=45^\circ$  in the cases of KCl, KBr and KI.

The potential map in (c) of each figure may describe the crystallization process, though only three chains are considered to align parallel each other as in the (010) plane of the  $\alpha$ -form. The calculation does not show the large difference in the potential energy in crystallizing polymer chains on the substrates. The c-axis of PPX crystallite should be nearly along the  $\langle 100 \rangle$  direction of substrate, since the values of  $\phi$  corresponding to the

potential minima are not largely different from  $0^\circ$  in the cases of KCl, KBr and KI. No defined minimum exists for NaCl, while the potential minima with the similar value are observed for KCl, KBr and KI. The difference in the degree of orientation observed experimentally is not elucidated from the calculation on the crystallization process.

From above, the orientation of the  $\alpha$ -form PPX is determined mainly by the polymerization stage. The epitaxial growth seems to take place independently of chain crystallization, because the rearrangement of polymer chains is considered to be prohibited during crystallization. The geometrical relation of KBr and PPX chain (cf. Figure 13-(b)) is shown in Figure 15.

#### ACKNOWLEDGEMENT

The author wishes to express his sincere gratitude to Professor K. Asai and Professor K. Katayama and Dr A. Kawaguchi for their encouragement in the course of this study. Thanks are due to Dr K. Kajiwara for his critical reading of the manuscript.

## REFERENCES

- 1) Willems.J ; Discussion Faraday Soc., 1957, 25, 111
- 2) Fischer.E.W.; Discussion Faraday Soc., 1957, 25, 204
- 3) Mauritz.K.A., Baer.E. and Hopfinger.A.J.; J Polym. Sci., Macromol. Reviews, 1978, 13, 1
- 4) Wunderlich.B.; "Macromolecular Physics" Academic Press, Chapter 3, 1973
- 5) Mauritz.K.A., Baer.E. and Hopfinger.A.J ; J Polym. Sci., Polym. Phys. 1973, 11, 2185  
Mauritz.K.A. and Hopfinger.A.J ; J. Polym. Sci., Polym. Phys., 1975, 13, 787  
Mauritz.K.A. and Hopfinger.A.J ; J Polym. Sci., Polym. Phys., 1976, 14, 1813
- 6) Macchi.E.M.; J. Polym. Sci., A-1, 1972, 10, 45
- 7) Rickert.S.E., Lando.J.B., Hopfinger.A.J and Baer.E.; Macromolecules, 1979, 12, 1053
- 8) Tsuji.M., Isoda.S., Ohara.M., Kawaguchi.A. and Katayama.K.; Polymer, 1982, 23, 1568
- 9) Niegisch.W.D.; J Appl. Phys., 1967, 38, 4110  
Kubo.S. and Wunderlich.B.; J. Appl. Phys., 1971, 42, 4558
- 10) Gorham.W.F ; J. Polym. Sci., A-1, 1966, 4, 3027
- 11) Pashley.D.W.; "Epitaxial Growth" ed. by Matthews.J.M., Academic Press 1975

- 12) Kubo.S. and Wunderlich.B.; J Polym. Sci., Polym. Phys., 1972, 10, 1949
- 13) Iwamoto.R., Bopp.R.C. and Wunderlich.B.; J Polym. Sci., Polym. Phys. 1975, 13, 1925
- 14) Iwamoto.R. and Wunderlich.B.; J. Polym. Sci., Polym. Phys., 1973, 11, 2403
- 15) Niegisch.W.D.; J Appl. Phys., 1966, 37, 4041
- 16) Miles.M. and Gleiter.H.; J Macromol. Sci.-Phys., 1978, B15, 613
- 17) Isoda.S., Tsuji.M., Ohara.M., Kawaguchi.A. and Katayama.K.; Polymer, in press
- 18) Isoda.S. and Katayama.K.; Polymer Preprints, Japan, 1982, 31, 854, submitted for publication
- 19) Pashley.D.W.; Advances in Physics, 1958, 5, 174
- 20) Kern.R., Lay.G.Le. and Metois.J.J ; "Current Topics in Material Science" vol.3 ed. by Kaldis.E. North-Holland 1979
- 21) Rybnikar.F and Geil.P.H.; J Polym. Sci., A-2, 1972, 10, 961
- 22) Wellinghoff.S., Rybnikar.F and Baer.E.; J Macromol. Sci.-Phys., 1974, B10, 1  
Rickert.S.E. and Baer.E.; J Appl. Phys., 1976, 47, 4304  
Rickert.S.E. and Baer.E.; J Materials Sci., 1978,

13, 451

- 23) Rickert.S.E., Ishida.H., Lando.J.B., Koenig.J.L. and Baer.E.; J Appl. Phys., 1980, 51, 5194
- 24) Wittmann.J.C. and Lotz.B.; J Polym. Sci., Polym. Phys., 1981, 19, 1837
- 25) Mayer.J.E.; J Chem. Phys., 1933, 1, 270
- 26) Hopfinger.A.J ; "Conformational Properties of Macromolecules" Academic Press 1973
- 27) Bondi.A.; J Phys. Chem., 1964, 68, 441
- 28) Pauling.L.; "The Nature of the Chemical Bond" Cornell Univ. Press 1960



Table 1. Misfit= $100(c-a)/a$ ; a is the a-axis dimension of a substrate, c the fiber period of PPX (0.655nm)

	NaCl	KCl	KBr	KI
a (nm)	0.563	0.629	0.660	0.707
misfit (%)	+16.3	+4.1	+0.8	-7.4

Table 2. The constants of the 6-12 potential.  $A_{ij}$  are given in units of  $10^{-6}$  kcal nm<sup>6</sup>/mole,  $B_{ij}$  of  $10^{-16}$  kcal nm<sup>12</sup>/mole

$i-j$	$A_{ij}$	$B_{ij}$
C-Na	107	1.55
H-Na	32.1	0.170
C-K	409	12.2
H-K	122.	1.57
C-Cl	893.	66.6
H-Cl	266.	11.3
C-Br	1160.	110.
H-Br	346.	16.6
C-I	1670	224.
H-I	496.	35.1

Table 3. Minimum potential energy at  $(\phi, h)$  is given in units of kcal/monomer mole.

	one monomer	one chain	three chains
NaCl	-5.4 $\phi = -13.5^\circ$ $h = 0.40\text{nm}$	not clear	not clear
KCl	-7.2 $\phi = -13.5^\circ$ $h = 0.375\text{nm}$	-5.8 $\phi = 0.0^\circ$ $h = 0.40\text{nm}$	-4.6 $\phi = -13.5^\circ$ $h = 0.44\text{nm}$
KBr	-7.5 $\phi = -13.5^\circ$ $h = 0.375\text{nm}$	-6.9 $\phi = 0.0^\circ$ $h = 0.38\text{nm}$	-4.5 $\phi = -4.5^\circ$ $h = 0.44\text{nm}$
KI	-7.3 $\phi = -13.5^\circ$ $h = 0.38\text{nm}$	-4.9 $\phi = 0.0^\circ$ $h = 0.43\text{nm}$	-4.3 $\phi = 0.0^\circ$ $h = 0.46\text{nm}$

#### FIGURE CAPTIONS

Figure 1. Schematic drawing of polymerization chamber. Dimer of p-xylylene is evaporated at a temperature between 80°C and 100°C, pyrolyzed at 650°C, polymerized and crystallized on the (001) plane of alkali halides at 25°C.

Figure 2. Electron diffraction patterns of as-polymerized PPX on (a) NaCl, (b) KCl, (c) KBr and (d) KI. The direction of electron beams is perpendicular to the surface of the PPX film. The vertical and horizontal directions in the figures are the  $\langle 100 \rangle$  and  $\langle 010 \rangle$  directions of substrates. Inner diffraction ring is the 020- and outer the 110-reflection of the  $\alpha$ -form. The stronger 110-reflections are oriented on the lines along the  $\langle 100 \rangle$  and  $\langle 010 \rangle$  directions of alkali halides.

Figure 3. Decoration pattern along curved 100 steps is frequently observed, when the very thin PPX film is shadowed by Pt-Pd; (a) on KI and (b) on KBr

Figure 4 Electron diffraction patterns and images of PPX films annealed at 380°C on (a) NaCl, (b) KCl, (c) KBr and (d) KI. Clear correlation with the substrates is

observed. The highest degree of epitaxy is obtained and correspondingly a well developed crosshatched structure is observed in the case of KBr

Figure 5. A high resolution lattice image in a crystallite of the PPX film annealed on KBr at 380°C. This image was taken with JEM-500 and processed by an optical filtering method. The lattice fringes correspond to the (001) spacing of the  $\beta$ -form PPX. The insert is an optical diffractogram from a crystallite in the original micrograph. The lattice fringes in each crystallite show one orientation, i.e., along the  $\langle 100 \rangle$  or  $\langle 010 \rangle$  direction of the substrate, and then the crosshatched structure is supposed to be as the right where rectangular crystallites aggregate perpendicularly each other. The arrows denote the chain directions in crystallites.

Figure 6 (a) For as-polymerized PPX, the (010) plane of the  $\alpha$ -form is parallel to the surface of substrate and the c-axis orients along the  $\langle 100 \rangle$  or  $\langle 010 \rangle$  direction of the substrate; (b) Electron diffraction pattern of annealed PPX is understood as overlapping of patterns with two molecular orientations which perpendicularly orient along the  $\langle 100 \rangle$  and  $\langle 010 \rangle$  directions of the

substrate. One of them is indexed as shown in the picture; (c) For annealed PPX, the (100) plane of the  $\beta$ -form is parallel to the surface of the substrate and the c-axis orients along the  $\langle 100 \rangle$  or  $\langle 010 \rangle$  direction of the substrate.

Figure 7 PPX single crystals grown from the dilute solution in  $\alpha$ -chloronaphthalene at 210°C. In the lath-shaped  $\alpha$ -form and the hexagonal-shaped  $\beta$ -form single crystals, the growth planes are the (010) plane of the  $\alpha$ -form and the (100) plane of the  $\beta$ -form.

Figure 8 (a) Electron diffraction pattern of PPX film annealed on KBr at 420°C. The original orientation observed in Figure 4 is largely disordered. (b) The smooth surface originally observed for the film annealed at 380°C develops into a block-like structure and the surface roughness is revealed by Pt-Pd shadowing.

Figure 9. Electron diffraction pattern of the PPX film polymerized and annealed at 380°C on KBr, previously covered with a thin carbon layer 3 nm thick. The chain axis is supposed to lie on the surface of the film by the fact that the 00<sup>l</sup>1-reflections are strong, but the c-axis

orientation along the  $\langle 100 \rangle$  or  $\langle 010 \rangle$  direction of the substrate was not observed.

Figure 10 The  $\langle 100 \rangle$  direction of the substrate is the u-axis, the  $\langle 010 \rangle$  the v-axis and the  $\langle 001 \rangle$  the h-axis. The origin of the coordinate is at one positive ion on the surface of substrate. In this coordinate, a center of a benzene ring in the polymer is  $(u,v,h)$ . The chain direction with respect to the u-axis is  $\phi$ ; (b) Potential calculation between i Atom in the polymer and j Ion in the substrate is done discretely in a hemisphere region with radius R and continuously in the rest region of the substrate; (c) u and v are changed in the shaded region OAB and the minimum of potential energy is obtained at a contact point P in each substrate.

Figure 11. Potential maps calculated for NaCl at the contact point P. Numbers in the figures are the values of potential energy in units of kcal/monomer mol. The minimum position is denoted by +; (a) Potential map for one monomer; (b) Potential map for one chain with seven monomers; (c) Potential map for three chains, each of which is composed with seven monomers.

Figure 12. Potential maps calculated for KCl at the contact point; (a) one monomer; (b) one chain; (c) three chains.

Figure 13. Potential maps calculated for KBr at the contact point; (a) one monomer; (b) one chain; (c) three chains.

Figure 14. Potential maps calculated for KI at the contact point; (a) one monomer; (b) one chain; (c) three chains.

Figure 15. The geometrical relation predicted from the calculation between KBr and the polymer with seven monomers; (a) The single PPX chain and the first layer of KBr are shown as a projection along the  $\langle 010 \rangle$  direction of substrate, where the small and large circles represent positive and negative ions, respectively. The large and small filled circles in the polymer represent carbon and hydrogen atoms; (b) A projection along the  $\langle 001 \rangle$  direction of substrate.



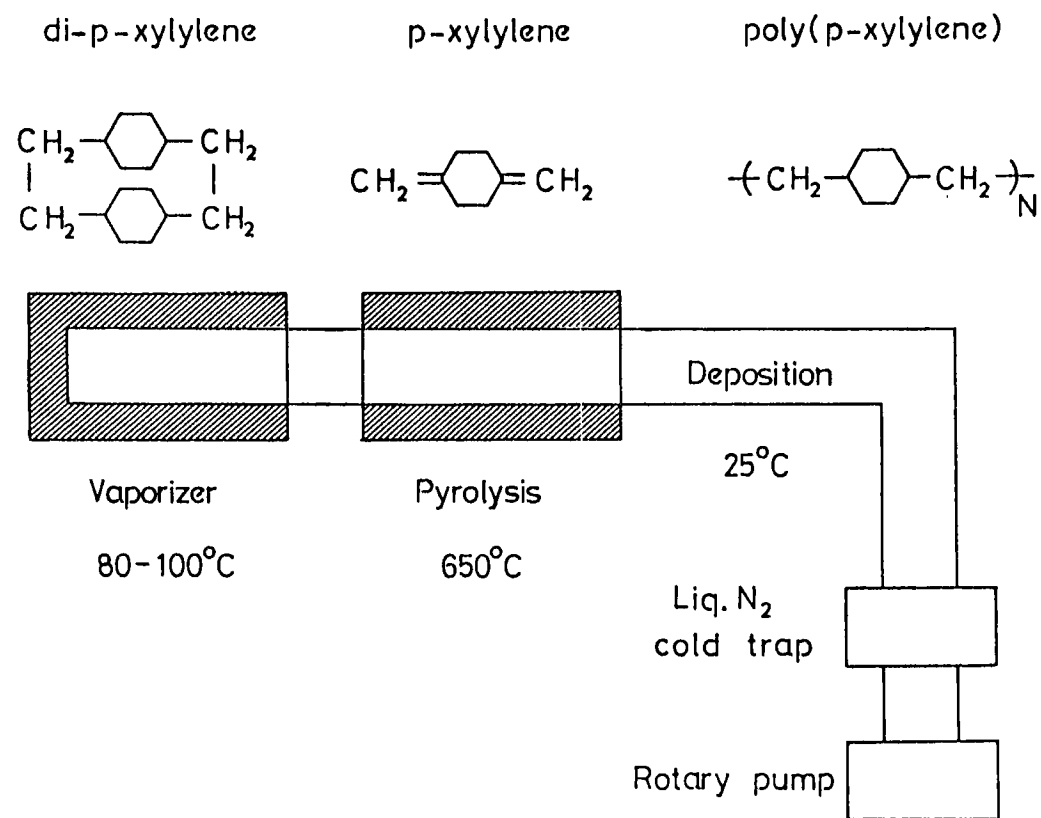


FIG. 1  
S I S O T A

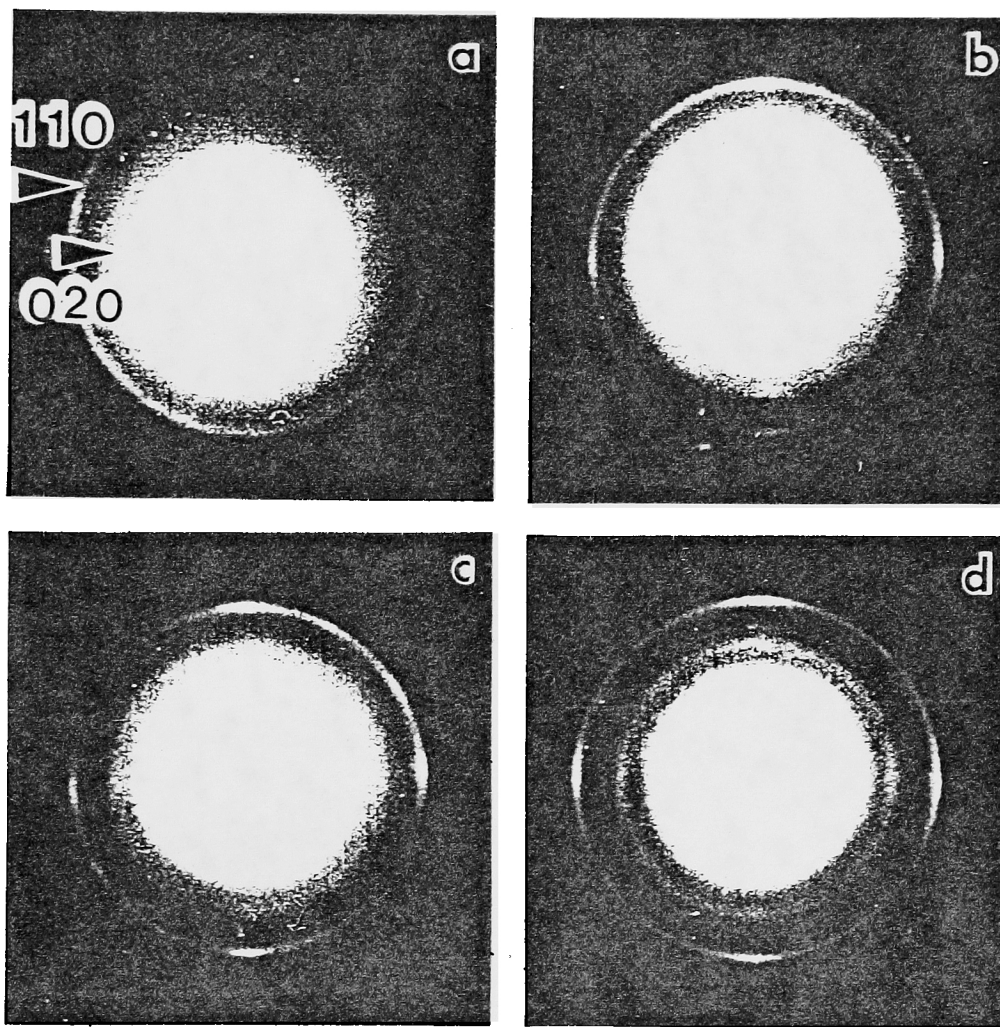


FIG. 2  
S. ISODA

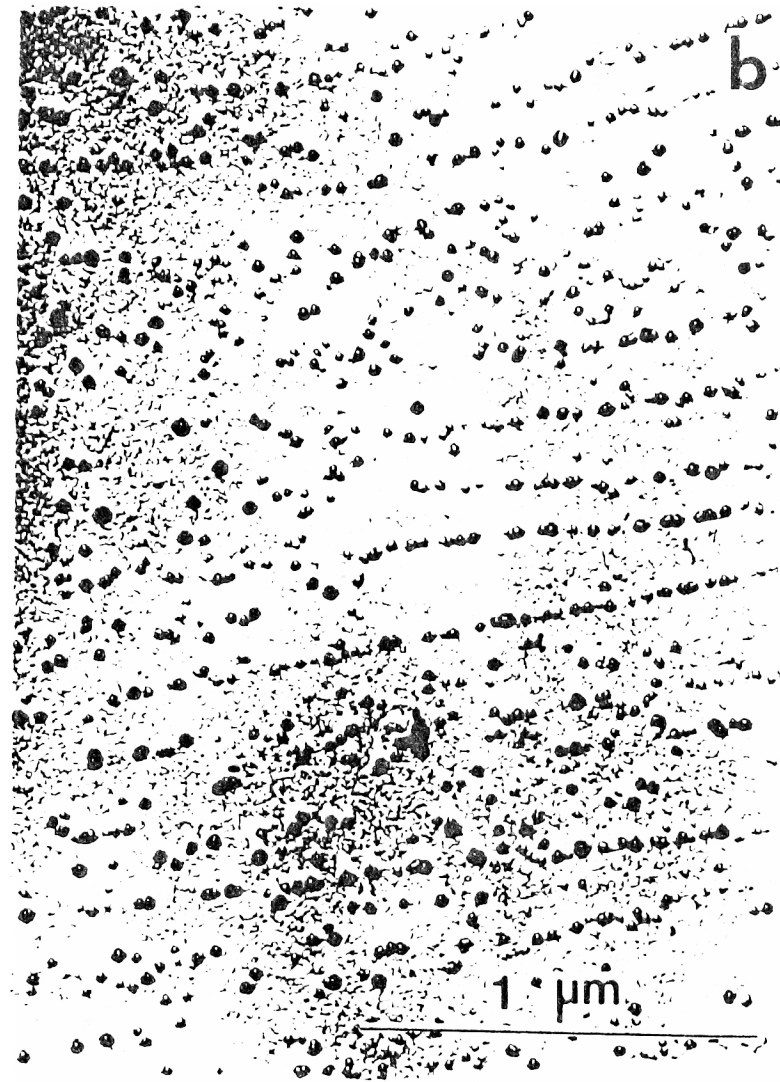
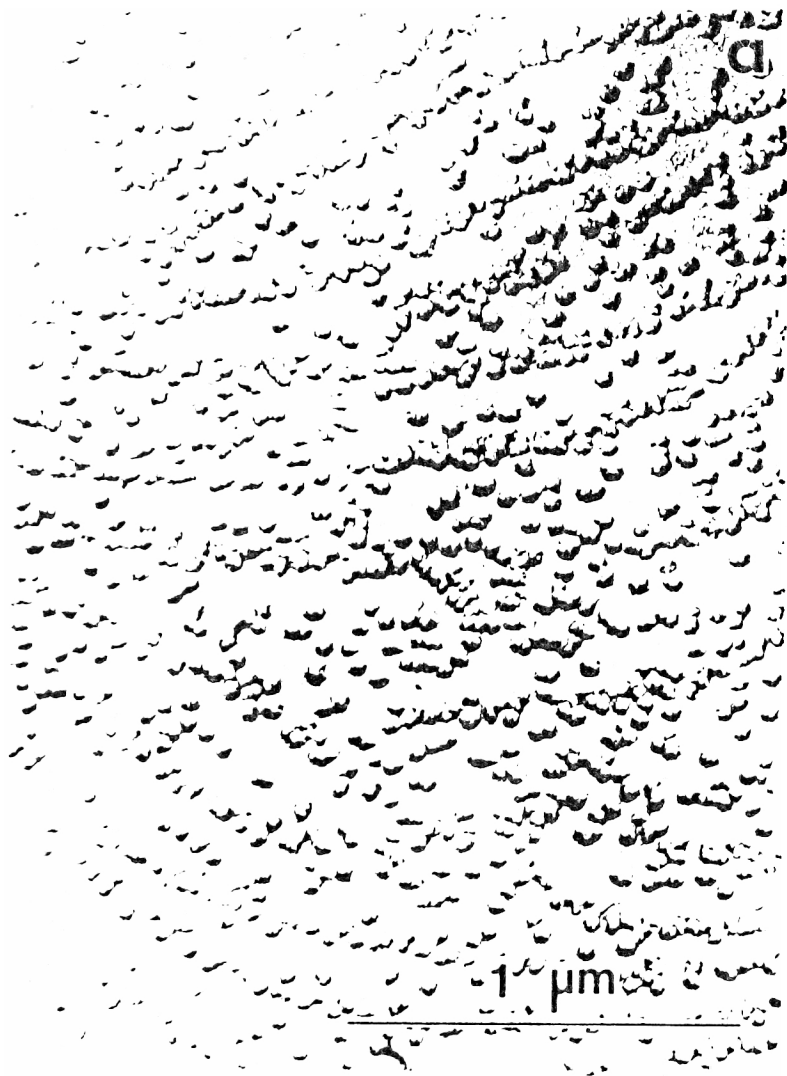


FIG. 3  
S. ISODA

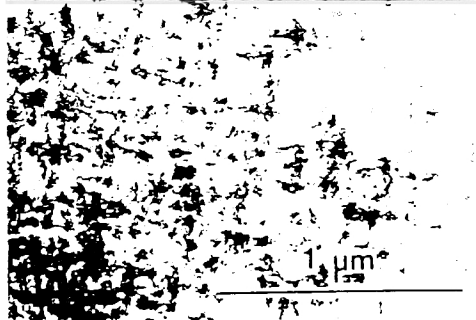
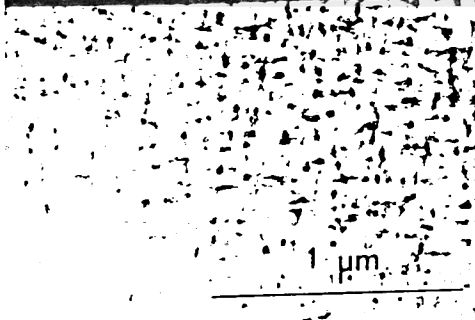
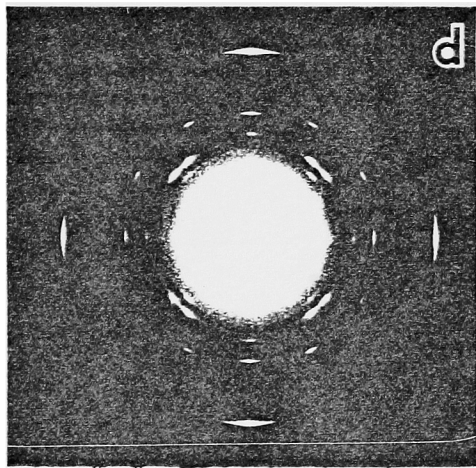
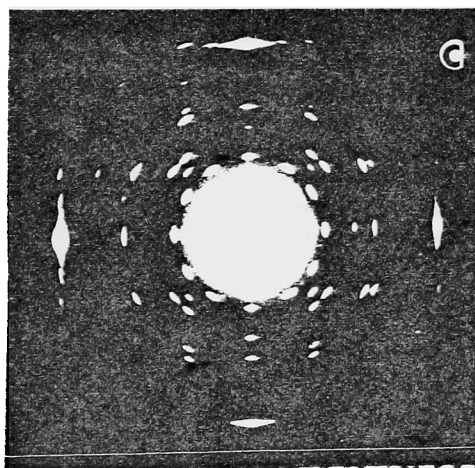
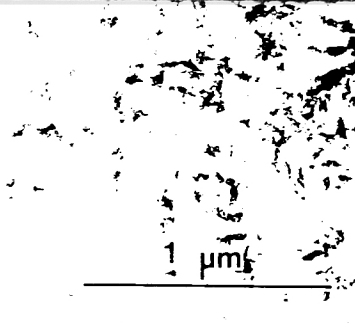
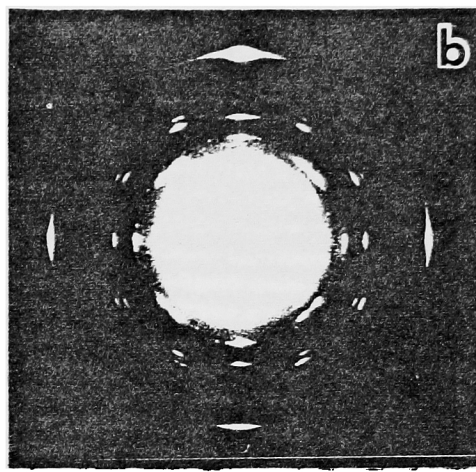
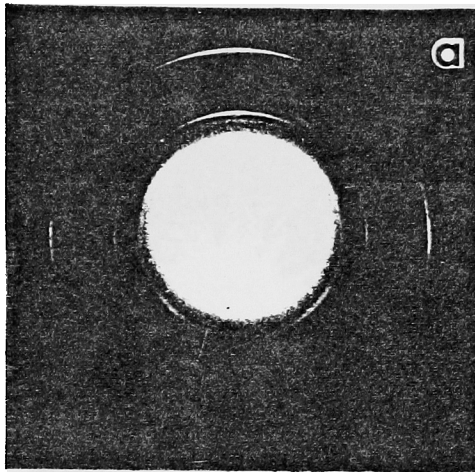


FIG. 4 S. ISODA

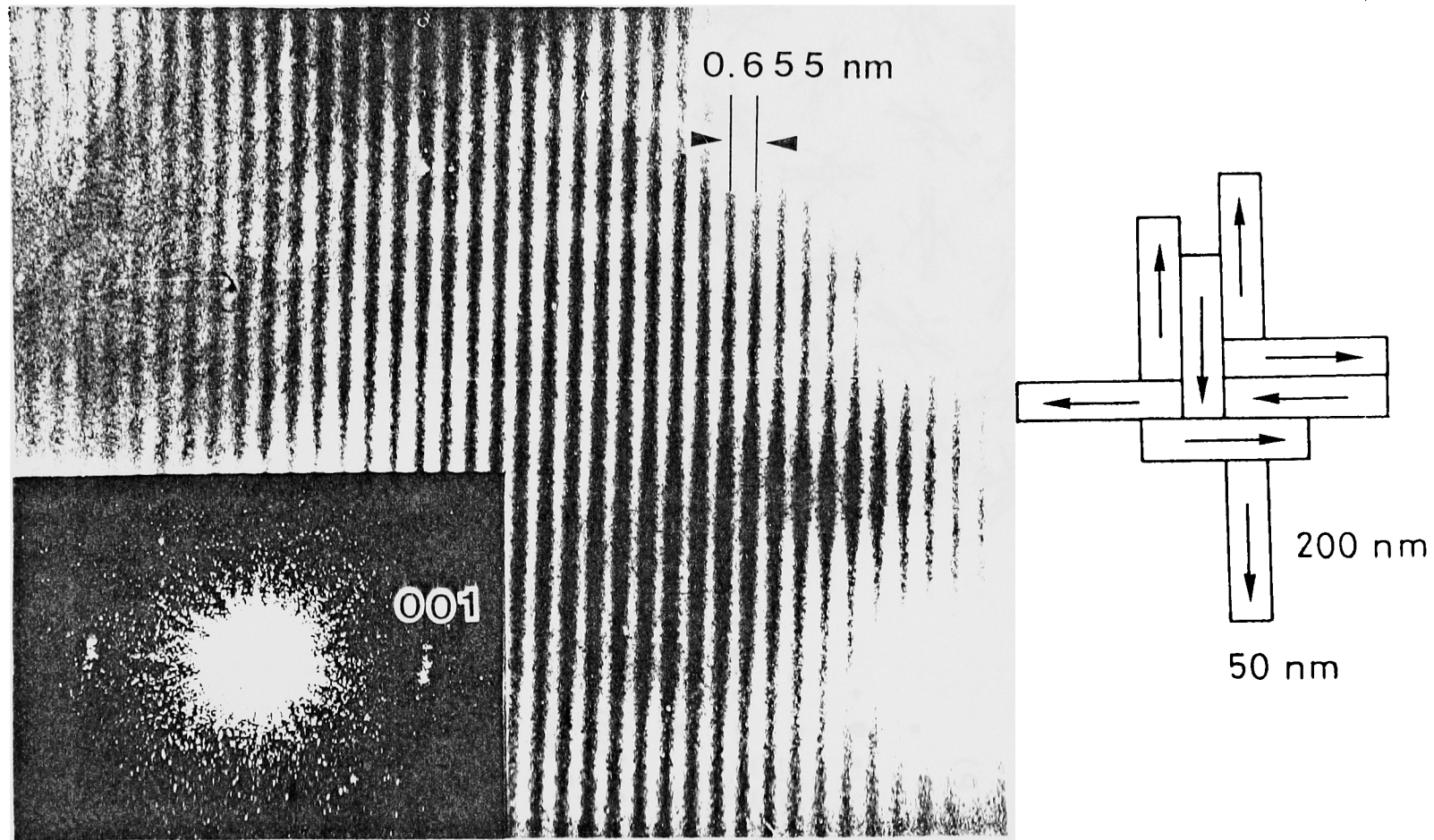
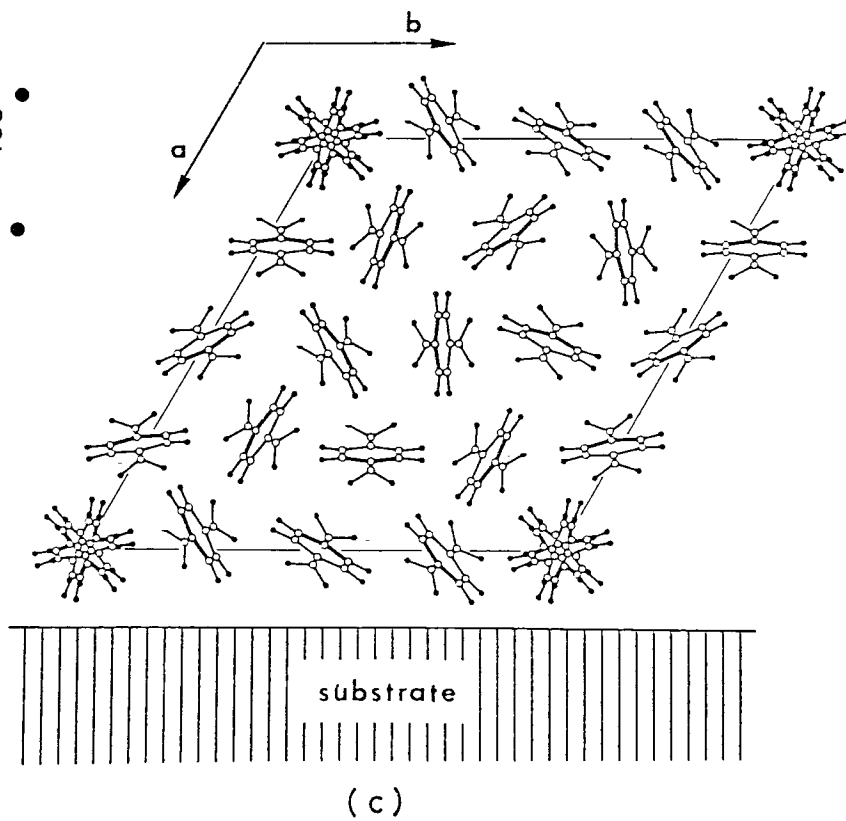
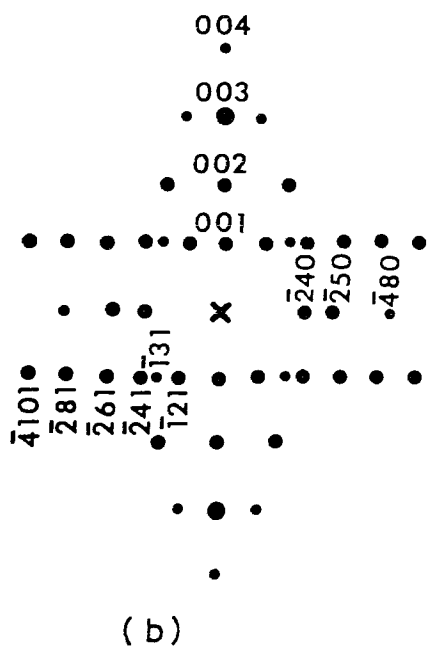
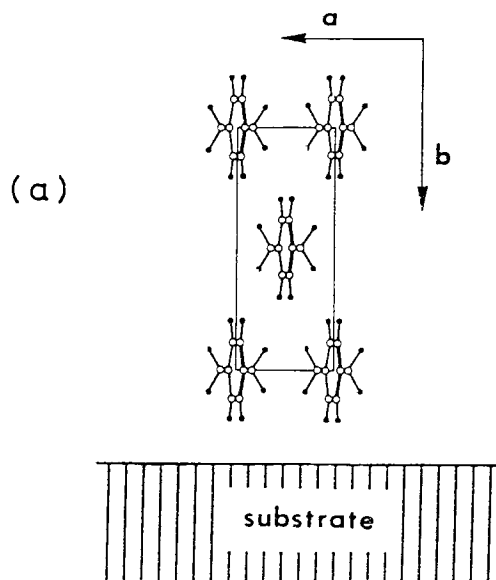


FIG. 5 S. ISODA

FIG. 6  
S. ISOPr



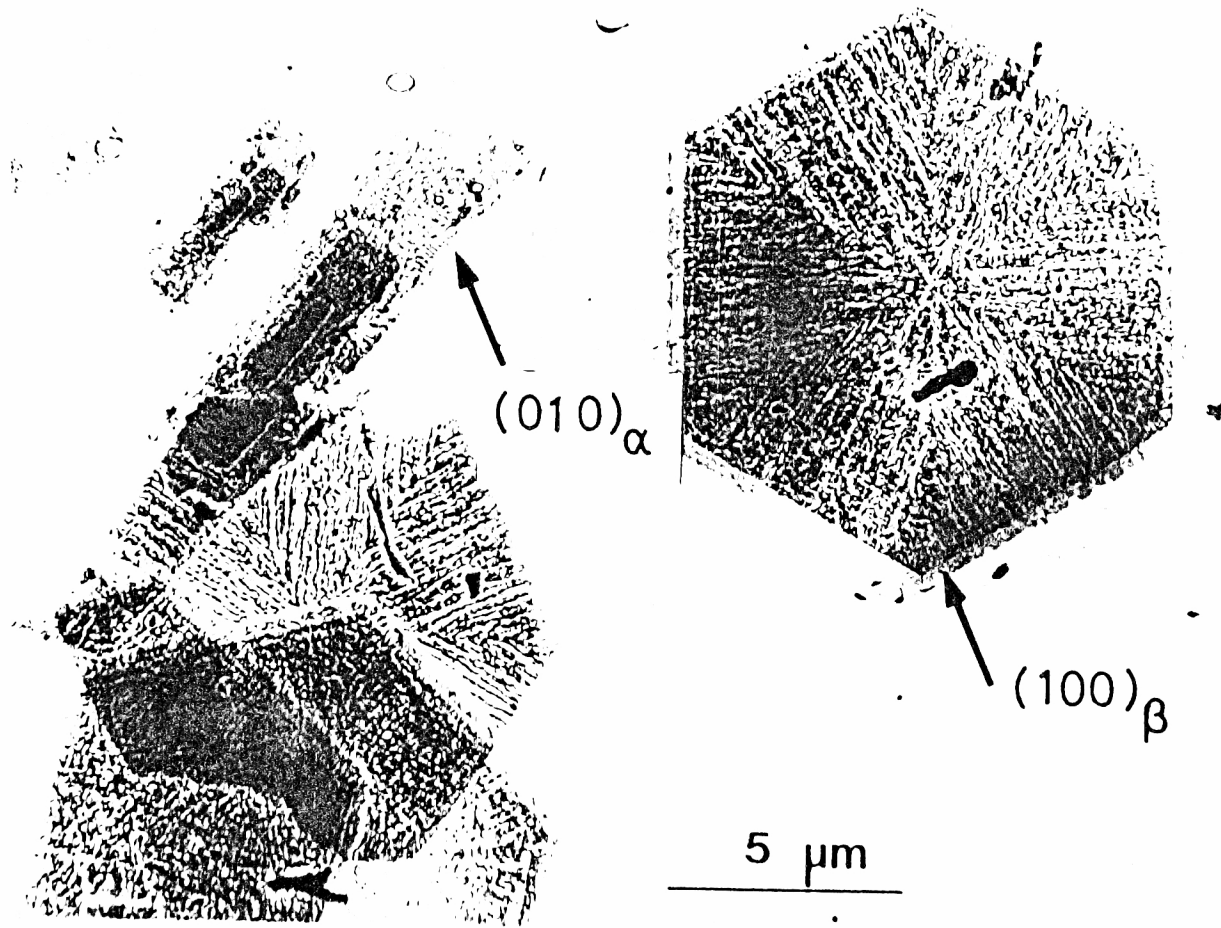


FIG. 7  
S. ISODA

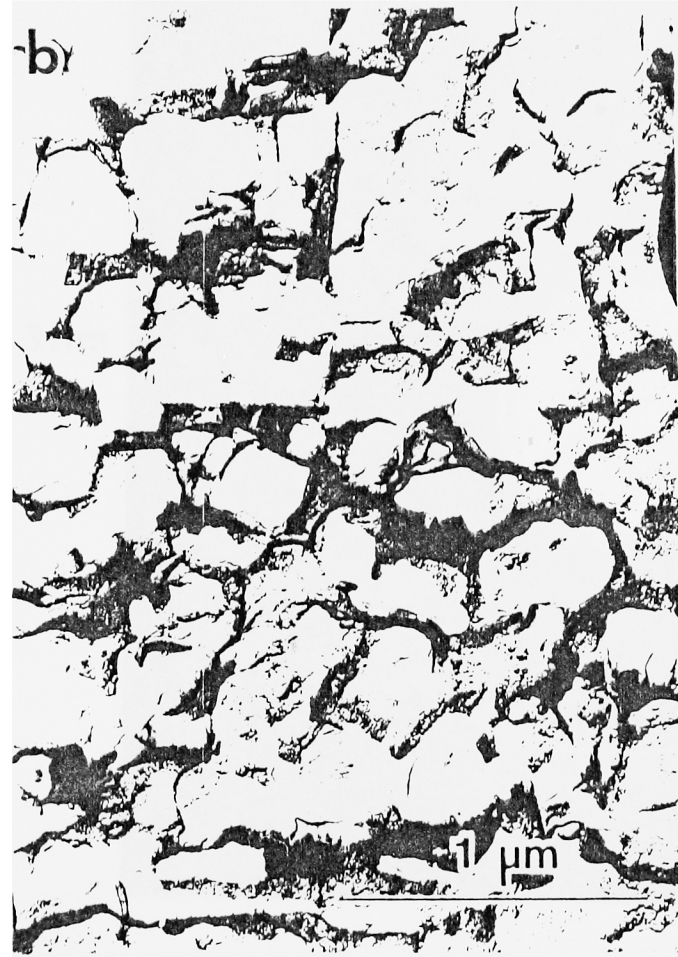
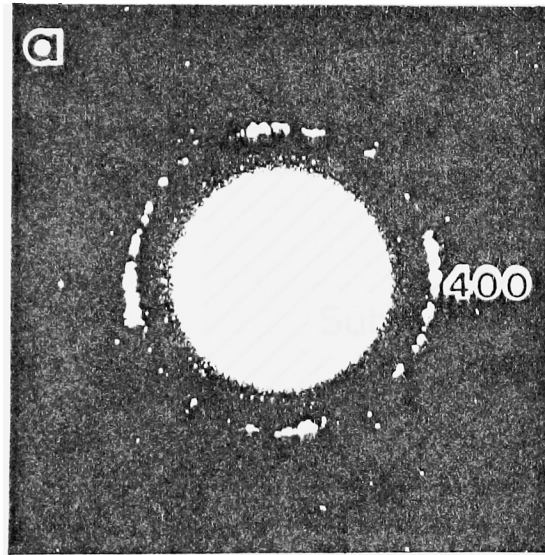


FIG. 8  
S. ISOPA



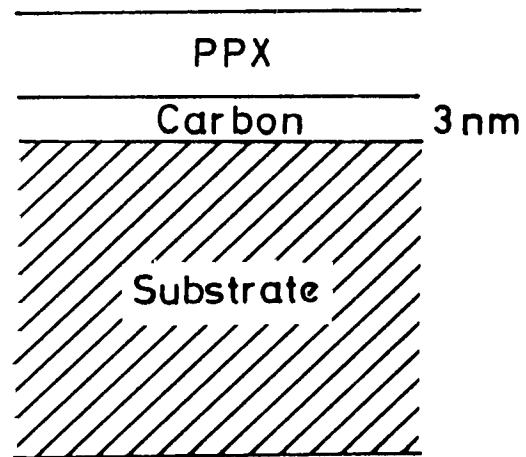
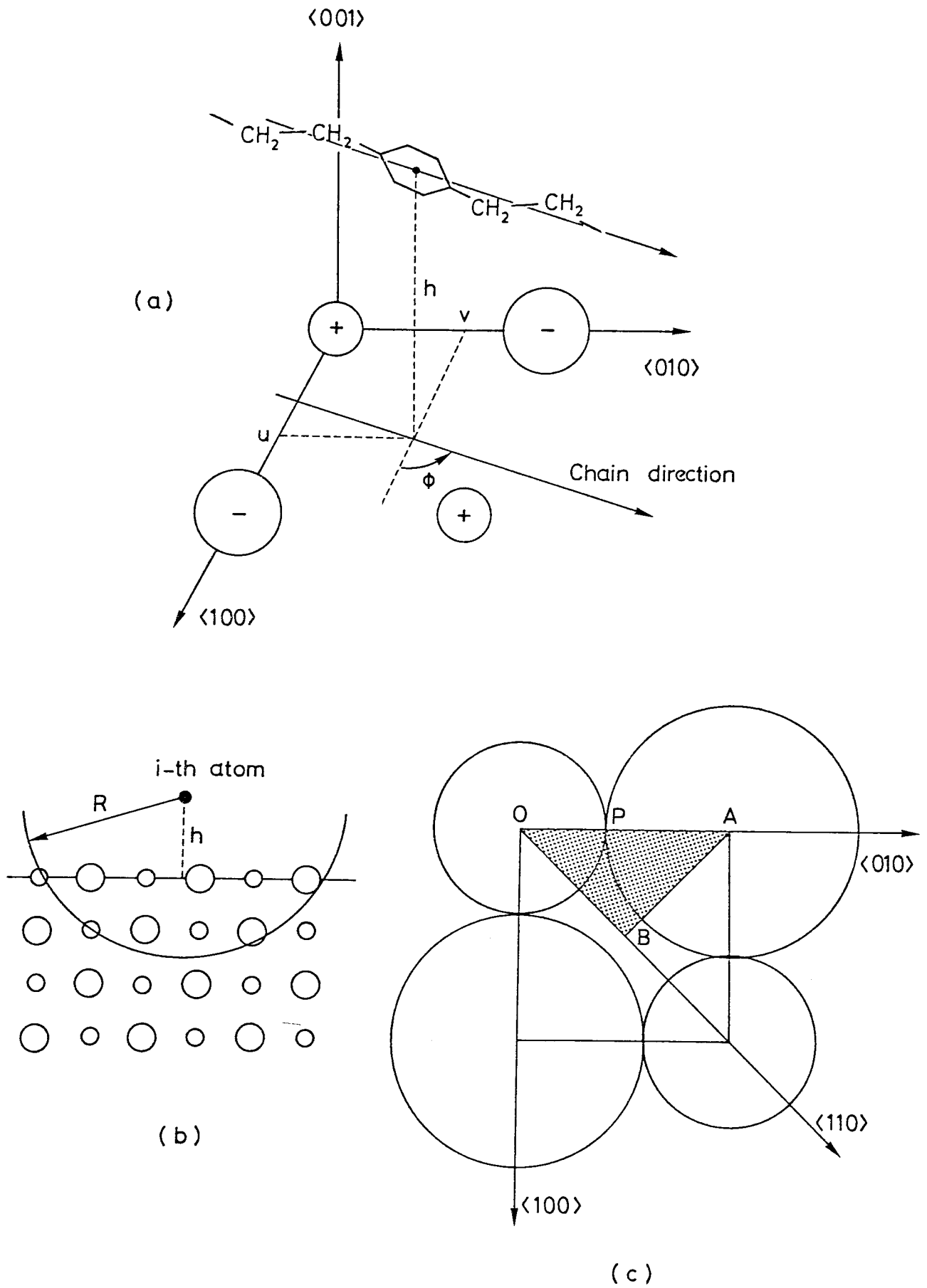


FIG. 9  
S. ISODA



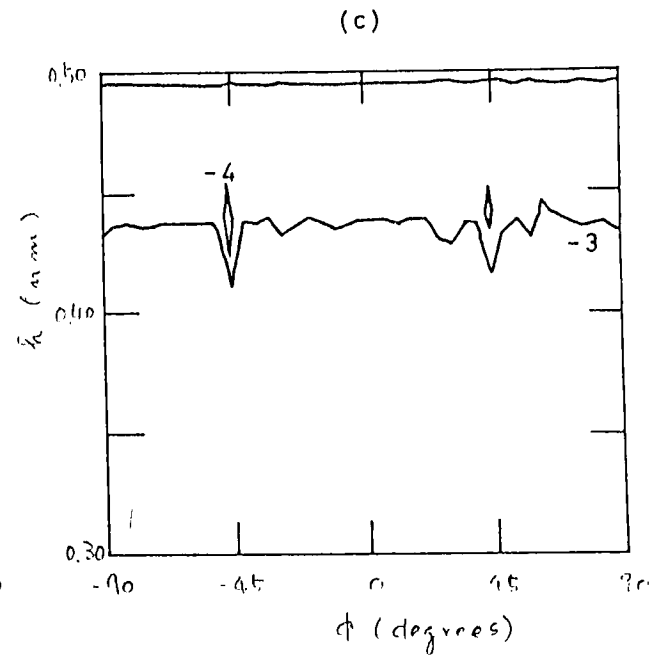
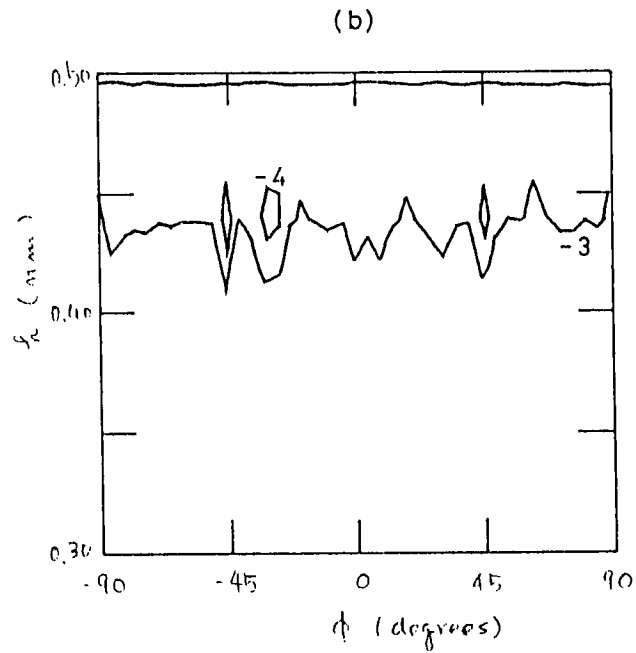
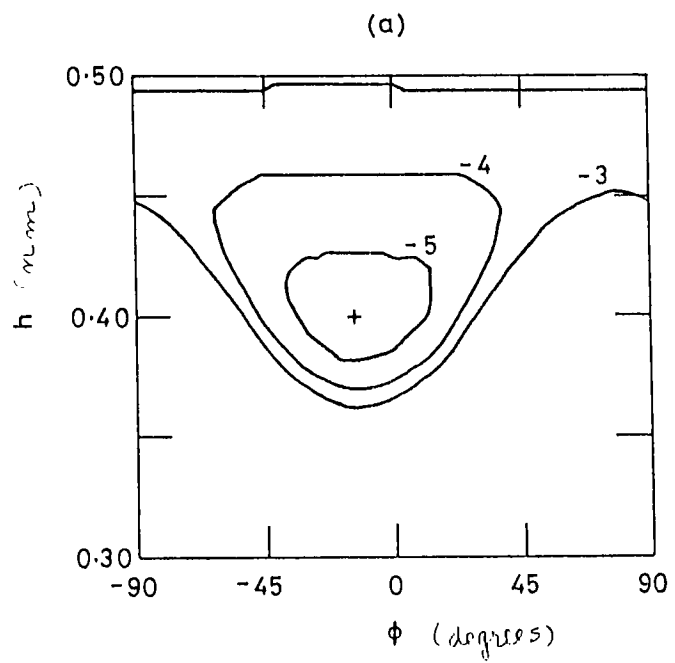


FIG. 11  
SISOVA

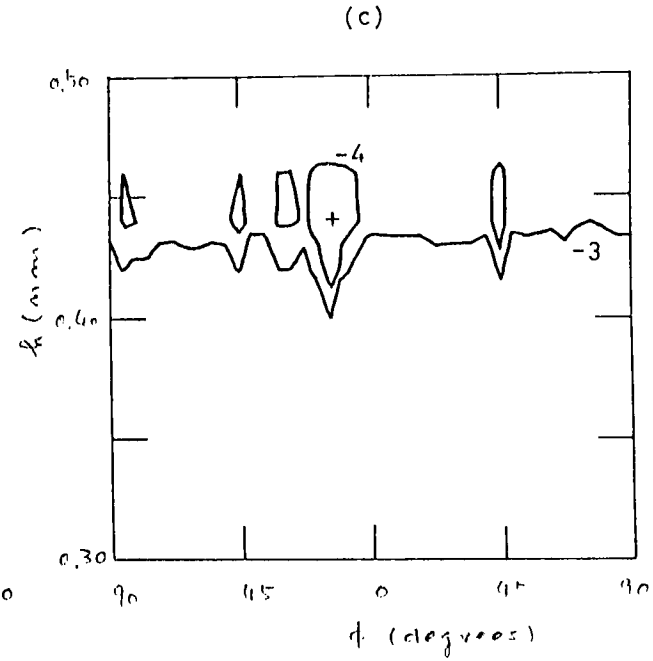
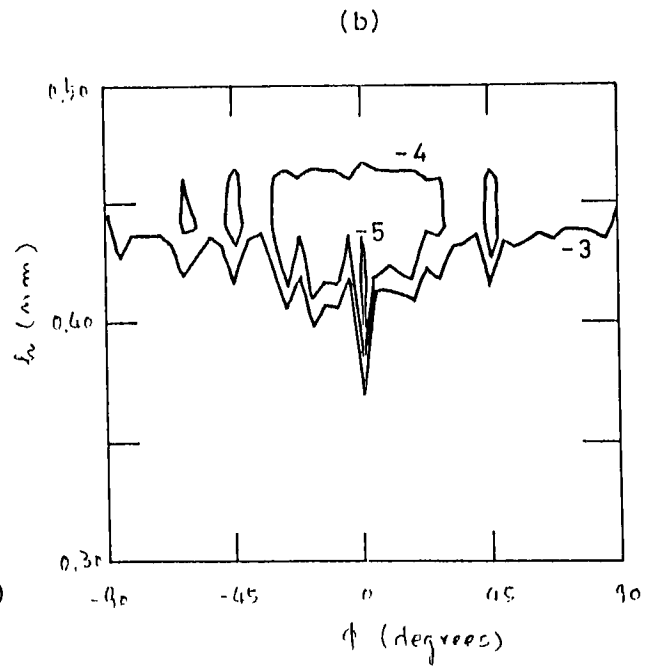
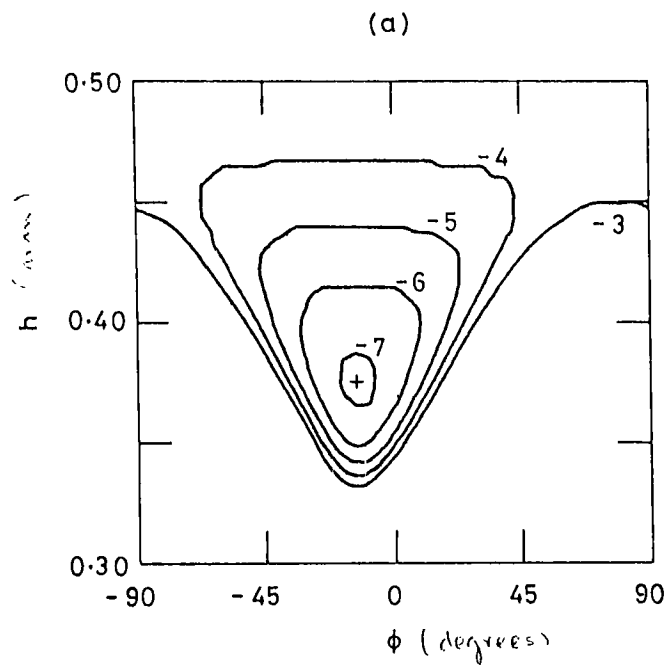


FIG 12  
S. ISODA

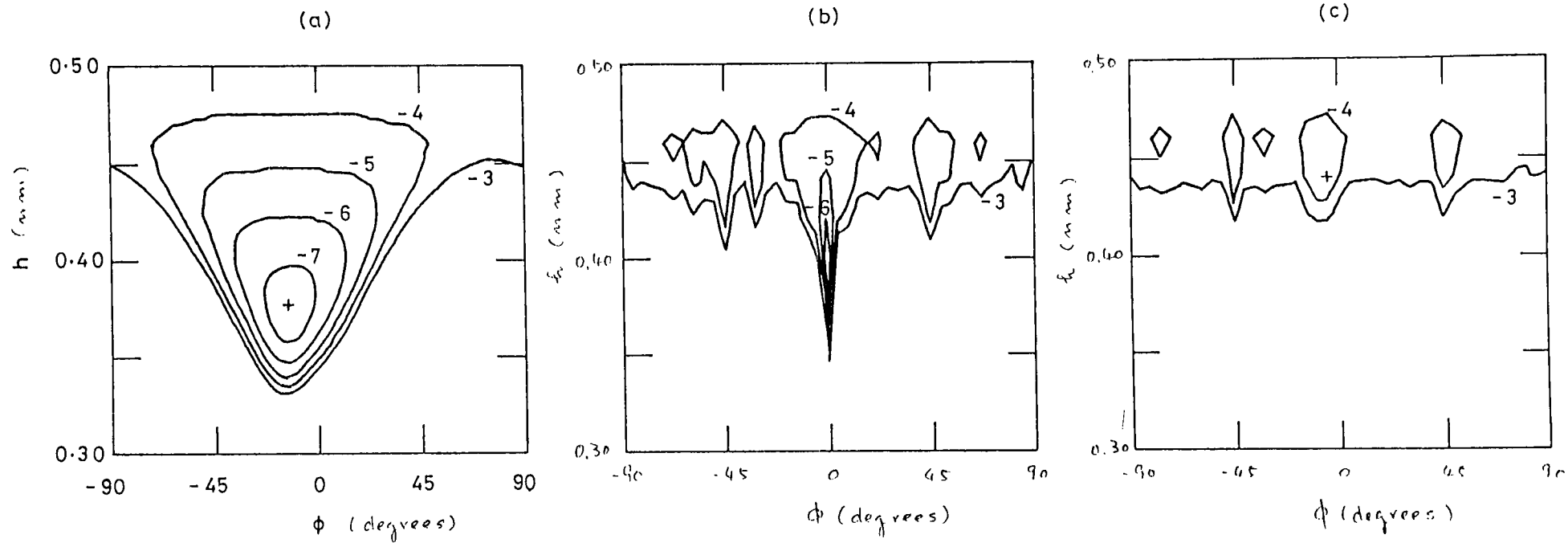


FIG 13  
S.I.S.C.D.A

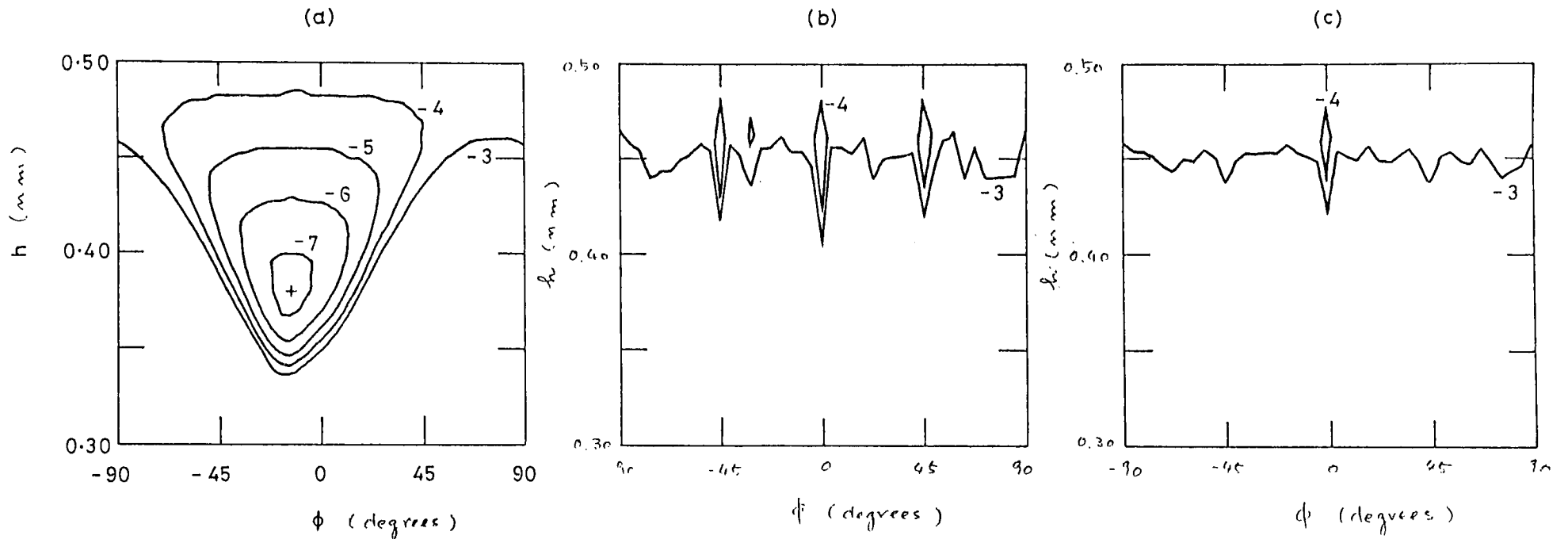
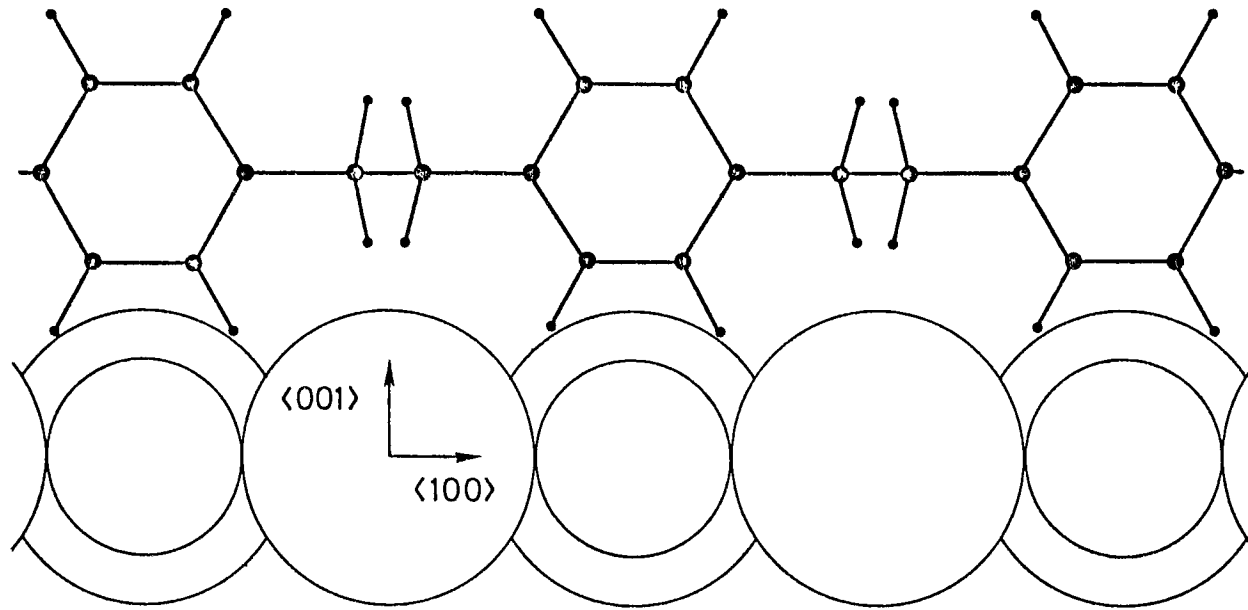


FIG. 1a  
S. ISODA

(a)



(b)

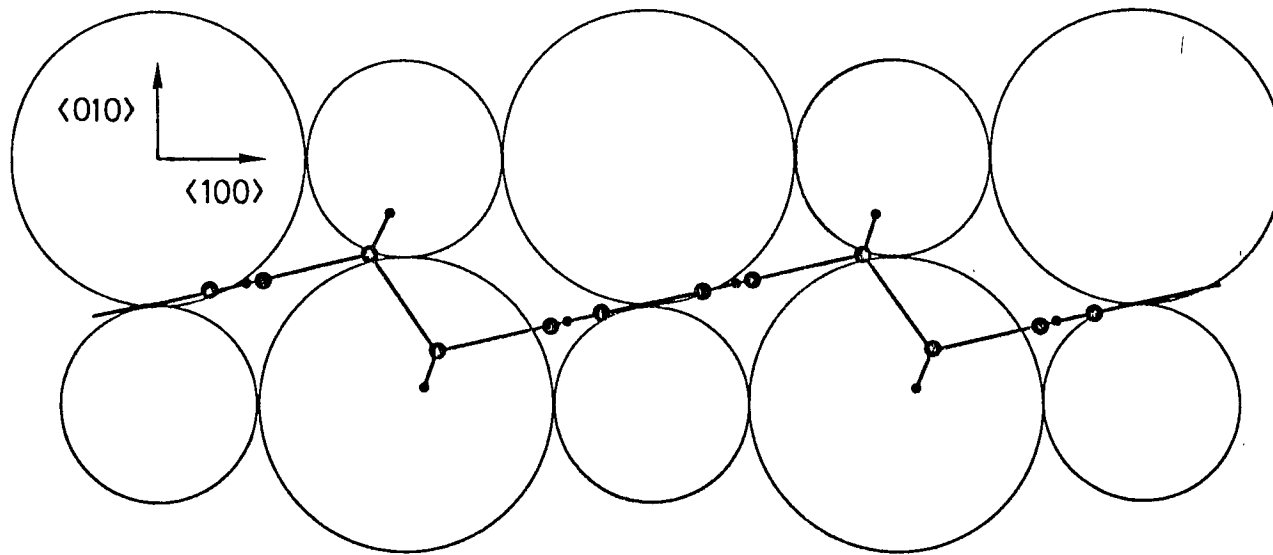


FIG. 15  
S. ISODA